

Published in final edited form as:

Nano Lett. 2010 November 10; 10(11): 4732-4737. doi:10.1021/nl103247v.

Time Resolved 3D Molecular Tracking in Live Cells

Nathan P. Wells 1,3 , Guillaume A. Lessard 1,4 , Peter M. Goodwin 1 , Mary E. Phipps 1 , Patrick J. Cutler 2 , Diane S. Lidke 2 , Bridget S. Wilson 2 , and James H. Werner 1

- ¹ Center for Integrated Nanotechnologies, Los Alamos National Laboratory, Los Alamos, NM 87545
- ² Department of Pathology, University of New Mexico Health Sciences Center, Albuquerque, NM 87131

Abstract

We report a method for tracking individual quantum dot (QD) labeled proteins inside of live cells that uses four overlapping confocal volume elements and active feedback once every 5 milliseconds to follow three dimensional molecular motion. This method has substantial advantages over 3D molecular tracking methods based upon CCD cameras, including increased Z tracking range (10 µm demonstrated here), substantially lower excitation powers (15 µW used here), and the ability to perform time-resolved spectroscopy (such as fluorescence lifetime measurements or fluorescence correlation spectroscopy) on the molecules being tracked. In particular, we show for the first time fluorescence photon anti-bunching of individual QD labeled proteins in live cells and demonstrate the ability to track individual dye labeled nucleotides (Cy5dUTP) at biologically relevant transport rates. To demonstrate the power of these methods for exploring the spatio-temporal dynamics of live cells, we follow individual QD-labeled IgE receptors both on and inside rat mast cells. Trajectories of receptors on the plasma membrane reveal three dimensional, nano-scale features of the cell surface topology. During later stages of the signal transduction cascade, clusters of QD labeled IgE-FceRI were captured in the act of ligand-mediated endocytosis and tracked during rapid (~950 nm/s) vesicular transit through the cell.

Keywords

Quantum Dot; Single Molecule; Fluorescence; Tracking; Microscopy; Cell

The direct observation of individual biological molecules in motion can transform our view of important biophysical and cellular processes. 1 For example, single molecule tracking has shed significant light on cellular membrane dynamics²⁻⁴, motor protein kinetics^{5, 6}, and gene regulation⁷. Advantages of a single molecule approach include the ability to observe dynamic, stochastic behavior (such as compartmentalized diffusion^{2, 4}) that would be masked in ensemble measurements and the ability for localization of molecules with a precision well below the diffraction limit of light⁵, ⁶. To date the field has primarily relied

SUPPORTING INFORMATION

Supporting information include Materials & Methods and a list of equations used for fitting and data analysis. Supporting figures include 3D tracking of individual fluorescent dyes (Cy5), and selected 3D trajectories of QD-IgE-FcERI on and inside antigenstimulated (Fig. S6-S8) and unstimulated (Fig. S5) mast cells. QuickTime movies, which show how the 3D trajectories of QD-IgE-FceRI evolve with time are available for all trajectories shown in the main text and in the supplementary information.

^{*}Corresponding Author: jwerner@lanl.gov.

3Current Address: Aerospace Corporation, Los Angeles, CA 90009

⁴Current Address: Covidien, Boulder, CO 80301

on wide-field imaging with a CCD camera, a method that generally captures spatio-temporal dynamics in only two dimensions.

While following the motion of individual molecules in two dimensions is a proven and powerful method to learn about biomolecular function, most aspects of life, including protein and RNA trafficking, inherently involve motion throughout three spatial dimensions. Unfortunately, tracking single molecules moving through three dimensions is a difficult, and until recently^{8–15}, unsolved technical problem. Many of the newly developed approaches to 3D molecular tracking use CCD cameras, either encoding Z information in their pointspread function^{8, 16} or follow the Z position with multiple cameras or image planes^{9, 14}. While these camera-based techniques can capture 3D molecular motion, they are generally limited in their Z-tracking range in cells to approximately plus or minus one µm from a fixed focal plane^{8, 10, 14, 17}, limited by the shallow depth of field of high numerical aperture microscope objectives needed for single molecule work. We point out the obvious: many cells are substantially thicker than two microns and different methods and techniques are required to follow single molecules throughout entire three dimensional cell volumes. In addition to its quite limiting Z-tracking range, CCD-based tracking approaches are also bounded in temporal resolution by the CCD frame rate (~1 ms for fast EM-CCDs), and must illuminate an entire cell slice at relatively large excitation intensities (~40 W/cm²).

In contrast to 3D molecular tracking based upon CCD cameras, 3D molecular tracking with confocal feedback $^{11-13,\ 15,\ 18}$ offers substantial advantages. First, the Z-tracking range is not limited by the depth of field of the objective (~1–2 μm), but rather is limited by the travel of the stage (10 μm) and ultimately limited by the working distance of the objective (~200 μm for the water immersion objective used here). This increase in Z-tracking range enables tracking biomolecular motion throughout the entire volume of many mammalian cells. Second, the temporal resolution is limited by the instrument response of a single element detector (~400 ps for single photon counting avalanche photodioes) and can thus potentially follow fast, dynamic motion on timescales orders of magnitude faster than CCDs 19 or perform time-resolved spectroscopy on the molecules being followed $^{11,\ 15}$. Third, as confocal excitation employs a tightly focused laser beam, whole-cell oxidative photo-damage is substantially less than it is for wide-field excitation.

Our previous investigations using 3D tracking via four overlapping confocal volume elements demonstrated one can follow individual quantum dots in three dimensions at biologically relevant transport rates¹³ and in high background environments¹⁵. Here we show the same 3D tracking method can be used to follow biomolecular traffic in live cells. In brief, our method uses four fiber optics as spatial filters (see Fig. 1) to simultaneously monitor four, near diffraction limited, points in the sample. Due to the arrangement and spacing of the fiber optics with respect to the tube lens of the microscope, the aggregate optical probe volume forms a three dimensional tetrahedron in the sample space. We note that even though the fiber optics have a small (~10 µm) gap between them (Fig. 1), the four detection volumes in the sample space overlap to a large extent (Figure S1 of the Supplementary Material). In particular, when a quantum dot is placed between two fibers, the sum of the counts for both detectors in a given image plane is only ~10% less than the sum of the counts obtained when the quantum dot is exactly centered on one of the figers (Fig. S1). When a single fluorescent molecule is present in the probe volume, active feedback of a fast XYZ piezo stage is used to keep the counts on all four photon detectors equal and as large as possible, with the stage position adjusted once every 5 msec. 15 The three dimensional localization accuracy for a single quantum dot in 5 msec is ~50 nm in X,Y and ~80 nm in Z, with the localization accuracy increasing approximately with the square root of the integration period (Figure S2), with . We note our approach to 3D molecular tracking is in many ways reminiscent of Berg's pioneering methods of following individual

bacteria during chemotaxis^{20, 21}, with the following exceptions: we employ 4 detectors (rather than 6) for 3D positional sensitivity, we use pulsed excitation and time-correlated single photon counting to record the arrival time of every photon detected with \sim 400 ps accuracy, and we can follow small, dim objects such as single quantum dots^{13, 15} or single organic dyes (see Figure 2).

As a model system for following biomolecular traffic in live cells, we take advantage of monovalent QD-IgE^{DNP} probes, previously shown to bind intact FcɛRI on the surface of the RBL-2H3 rat tumor mast cell line without perturbing the activation state of the receptor.⁴ Crosslinking of multiple QD-IgE-FcɛRI complexes with polyvalent ligand (DNP²⁴-BSA) leads to receptor activation, inducing a complex tyrosine kinase cascade and release of histamine and other inflammatory mediators.²² FcɛRI cross linking also induces marked changes in cell morphology, including extensive membrane ruffling²³ and receptor internalization.²⁴

Figure 3 and supplementary movie SM3 show a 3D trajectory of a single QD-labeled IgE-Fc ϵ RI complex on the side of an un-stimulated mast cell at 37°C. This trajectory shows we can follow motion over several microns in the Z-dimension (Fig 3A, 3D) and also highlights the time-resolved spectroscopies that can be performed while tracking (Fig 3F–H). During the ~14 sec observation period, the QD-IgE-Fc ϵ RI motion follows a complex 3D topology on the side of the mast cell that includes motion over 4 microns in the Z-direction (Fig. 3A, 3D). The mean squared displacement (MSD; Fig. 3E, blue) for this trajectory shows highly corralled diffusion (with a corral size of ~1.6 μ m), with fits to the early portion of the MSD revealing an inter-corral (or instantaneous) diffusion rate of 0.21 μ m²/sec, which is slightly faster than previous measurements of IgE-Fc ϵ RI diffusion on the basal membrane surface.⁴

In addition to recording the entire XYZ trajectory for this single molecule, the arrival time of every photon is recorded with ~400 ps time resolution. Recording the arrival times of individual photons opens the door to time-resolved analysis methods impossible with conventional CCD cameras. Three methods of analyzing this data are shown in Fig. 3F-H. Fig. 3F shows a histogram of the delay times between adjacent detected photons (a pair correlation measurement), showing fluorescence photon anti-bunching^{25, 26} from a single quantum dot undergoing motion on a live cell (the central peak is non-zero due to the background cellular auto-fluorescence ^{15, 27}). The fact the photons are anti-bunched in time (i.e. we infrequently detect 2 photons simultaneously) is a rigorous demonstration this track is of a single quantum system. ²⁵, ²⁶ Another means of analyzing the raw photon data is to construct a histogram of photon arrival times with respect to the laser pulse (Fig. 3G), which measures the fluorescence lifetime of the QD. Here we show the histogram for the entire trajectory, but we have previously shown this information can also be obtained as a function of time/molecule position. ¹⁵ In Fig. 3H, fluorescence correlation spectroscopy (FCS)²⁸ is used to analyze the fluctuations in emission intensity observed during the trajectory, with the correlation decay for this trajectory being dominated by QD blinking.²⁹ FCS is a powerful analysis method to observe bio-molecular conformational fluctuations^{30, 31} or to probe dynamics in live cells³², ³³. However, in general, observation times for most FCS measurements are limited to the transit of the molecule through the optical probe volume (~ 10 ms or less). Here, we demonstrate FCS can be performed on the same molecule in a live cell for an extended time period, even while this molecule is moving at biological transport

In addition to the temporal resolution afforded by confocal 3D tracking, the path of single QD-IgE-FcɛRI can map out complex 3D nanostructured topologies on cell surfaces³⁴, as demonstrated in Figure 4. During the first 25 seconds, the motion of this receptor is essentially two dimensional, with this 2D surface (the cell membrane) being nearly

perpendicular to the XY plane. However, this receptor then ventures perpendicular to cell membrane it has previously been confined to, mapping out a complex 3D nano-topology (most likely a cellular filopodia). Another example of 3D tracking mapping out 3D membrane topology is given by Supplementary Figure S6 and Movie SM6, which show a the 3D trajectory for a single QD-IgE-FceRI on a highly curved region of the plasma membrane.

While our ability to follow individual quantum dot labeled IgE-Fc ϵ RI receptors is usually limited by long-lived (>10 ms) dark states (i.e. QD blinking ^{15, 29}), aggregated, cross-linked clusters of multiple IgE-Fc ϵ RI receptors (each labeled with a QD) can be followed for very long time periods (several minutes). This is shown in Figure 5 and Movie SM5, where a cluster of ~5 QD-IgE-Fc ϵ RI receptors travels on the apical cell membrane for several minutes after the addition of antigen. Changes in the Z position during this phase are consistent with travels across a ruffled landscape²³ created by dynamic rearrangement of the underlying actin cytoskeleton. At ~250 seconds into observation, the receptor complex is taken up into an endocytic vesicle, plunging nearly 7 μ m into the cell interior and reaching an average velocity of 950 nm/sec during this transport event, consistent with previous measures of endocytic transport rates³⁵. Additional examples of large-scale Z directional motion in QD-IgE-Fc ϵ RI complexes, observed in antigen-stimulated RBL-2H3 cells, are found in the Supplemental section (Fig. S7, S8, S9 and Movie SM7, SM8, SM9).

In summary, we have demonstrated a confocal tracking method capable of following individual quantum dot labeled signaling molecules, in 3 dimensions, on and inside living cells. Trajectories can be measured for minutes and can extend up to 10 microns in all spatial dimensions, enabling tracking throughout the entire volume of many mammalian cells. In addition to the substantial kinetic data obtained from these three dimensional trajectories, individual photon arrival times are recorded with ~400 ps accuracy, enabling a number of time-resolved analysis methods impossible with camera-based tracking methods.

Supplementary Material

Refer to Web version on PubMed Central for supplementary material.

Acknowledgments

This work is supported by the National Institutes of Health (No. R21AI07707) and was performed at the Center for Integrated Nanotechnologies, a U.S. Department of Energy, Office of Basic Energy Sciences user facility. Los Alamos National Laboratory is operated by Los Alamos National Security, LLC, for the National Nuclear Security Administration of the U.S. Department of Energy under contract DE-AC52-06NA25396.

References

- 1. Pinaud F, Clarke S, Sittner A, Dahan M. Nat Methods. 2010; 7(4):275–285. [PubMed: 20354518]
- Fujiwara T, Ritchie K, Murakoshi H, Jacobson K, Kusumi A. J Cell Biol. 2002; 157(6):1071–1081.
 [PubMed: 12058021]
- 3. Dahan M, Levi S, Luccardini C, Rostaing P, Riveau B, Triller A. Science. 2003; 302(5644):442–5. [PubMed: 14564008]
- 4. Andrews NL, Lidke KA, Pfeiffer JR, Burns AR, Wilson BS, Oliver JM, Lidke DS. Nat Cell Biol. 2008; 10(8):955–963. [PubMed: 18641640]
- 5. Gelles J, Schnapp BJ, Sheetz MP. Nature. 1988; 331(6155):450–453. [PubMed: 3123999]
- Yildiz A, Forkey JN, McKinney SA, Ha T, Goldman YE, Selvin PR. Science. 2003; 27(300):2061– 2065. [PubMed: 12791999]
- 7. Elf J, Li GW, Xie XS. Science. 2007; 316(5828):1191–1194. [PubMed: 17525339]
- 8. Holtzer L, Meckel T, Schmidt T. Appl Phys Lett. 2007; 90:053902.

9. Toprak E, Balci H, Blehm BH, Selvin PR. Nano Lett. 2007; 7(7):2043–2045. [PubMed: 17583964]

- 10. Thompson MA, Lew MD, Badieirostami M, Moerner WE. Nano Lett. 2010:2775-2783.
- 11. McHale K, Berglund AJ, Mabuchi H. Nano Lett. 2007; 7(11):3535–3539. [PubMed: 17949048]
- 12. Cang H, Xu C, Montiel D, Yang H. Optics Letters. 2007; 32(18):2729–2731. [PubMed: 17873950]
- 13. Lessard G, Goodwin PM, Werner JH. Appl Phys Lett. 2007; 91(22):2224106.
- Ram S, Prabhat P, Chao J, Ward ES, Ober RJ. Biophys J. 2008; 95(12):6025–6043. [PubMed: 18835896]
- 15. Wells NP, Lessard GA, Werner JH. Anal Chem. 2008; 80:9830–9834. [PubMed: 19072277]
- 16. Thompson M, Lew M, Badieirostami M, Moerner W. Nano Lett. 10(1):211–218. [PubMed: 20000821]
- 17. Mlodzianoski M, Juette M, Beane G, Bewersdorf J. Optics Express. 2009; 17(10):8264–8277. [PubMed: 19434159]
- 18. Levi V, Ruan QQ, Gratton E. Biophys J. 2005; 88(4):2919–2928. [PubMed: 15653748]
- Sahl S, Leutenegger M, Hilbert M, Hell S, Eggeling C. PNAS. 2010; 107(15):6829. [PubMed: 20351247]
- 20. Berg HC. Rev Sci Instr. 1971; 42:868.
- 21. Berg HC, Brown DA. Nature. 1972; 239(5374):500. [PubMed: 4563019]
- 22. Andrews N, Pfeiffer J, Martinez A, Haaland D, Davis R, Kawakami T, Oliver J, Wilson B, Lidke D. Immunity. 2009; 31(3):469–479. [PubMed: 19747859]
- 23. Pfeiffer J, Seagrave J, Davis B, Deanin G, Oliver J. J Cell Biol. 1985; 101(6):2145. [PubMed: 2933414]
- 24. Barker S, Caldwell K, Hall A, Martinez A, Pfeiffer J, Oliver J, Wilson B. Molecular Biology of the Cell. 1995; 6(9):1145. [PubMed: 8534912]
- 25. Kimble HJ, Dagenais M, Mandel L. Phys Rev Lett. 1977; 39(11):691-695.
- Michler P, Imamoglu A, Mason MD, Carson PJ, Strouse GF, Buratto SK. Nature. 2000; 406(6799):968–970. [PubMed: 10984045]
- 27. Weston KD, Dyck M, Tinnefeld P, Muller C, Herten DP, Sauer M. Anal Chem. 2002; 74(20): 5342–5349. [PubMed: 12403591]
- 28. Magde D, Elson EL, Webb WW. Biopolymers. 1974; 13(1):29–61. [PubMed: 4818131]
- 29. Nirmal M, Dabbousi BO, Bawendi MG, Macklin JJ, Trautman JK, Harris TD, Brus LE. Nature. 1996; 383(6603):802–4.
- 30. Werner JH, Joggerst R, Dyer RB, Goodwin PM. PNAS. 2006; 103(30):11130–11135. [PubMed: 16844777]
- 31. Bonnet G, Krichevsky O, Libchaber A. PNAS. 1998; 95(15):8602. [PubMed: 9671724]
- 32. Bacia K, Kim SA, Schwille P. Nat Methods. 2006; 3(2):83–89. [PubMed: 16432516]
- 33. Eggeling C, Ringemann C, Medda R, Schwarzmann G, Sandhoff K, Polyakova S, Belov VN, Hein B, Von Middendorff C, Schonle A, Hell SW. Nature. 2008; 457(7233):1159–1162. [PubMed: 19098897]
- 34. Wells NP, Lessard GA, Phipps ME, Goodwin PM, Lidke DS, Wilson BS, Werner JH. Proc of the SPIE. 2009; 7185:7185-1–7185-13.
- 35. Nan X, Sims P, Chen P, Xie X. J Phys Chem B. 2005; 109(51):24220–24224. [PubMed: 16375416]

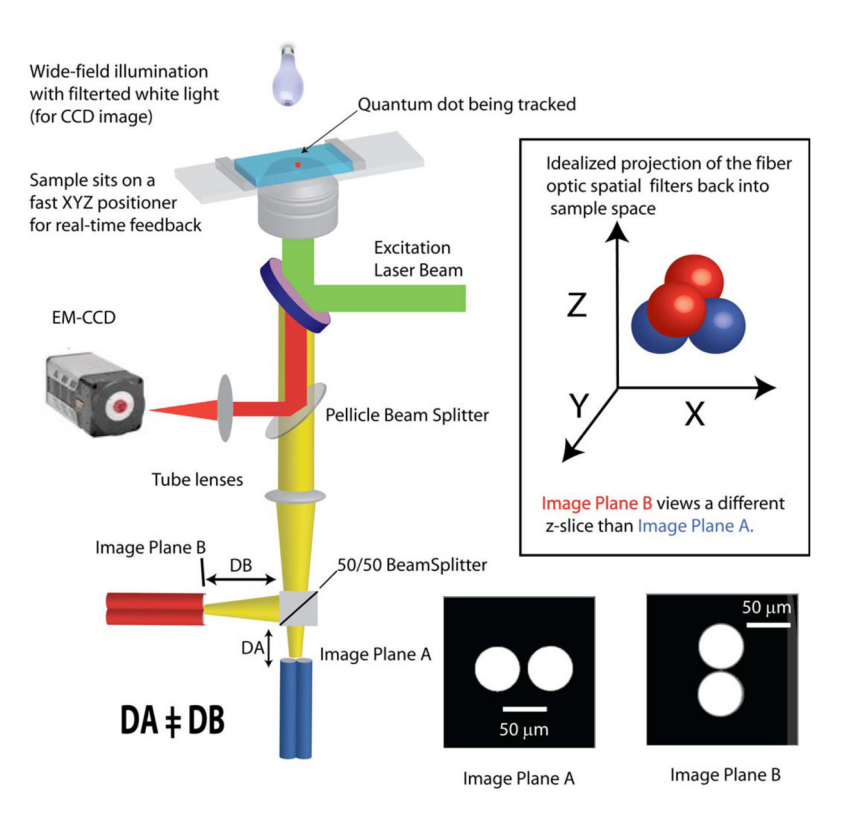


Figure 1. Schematic of the 3D tracking apparatus. Four fiber optics serve as spatial filters to examine four nearly diffraction limited spots in the sample simultaneously. Due to the spacing and arrangement of the fibers, these four spots form a 3D tetrahedron in the sample space. While tracking, active feedback of a XYZ piezo stage is used to keep counts on all four detectors equal and as large as possible. A small fraction (~8%) of the emission from the quantum dot receptor being tracked is sent to an EM-CCD camera, which enables contextual information for the position of the molecule in the cell during 3D tracking.

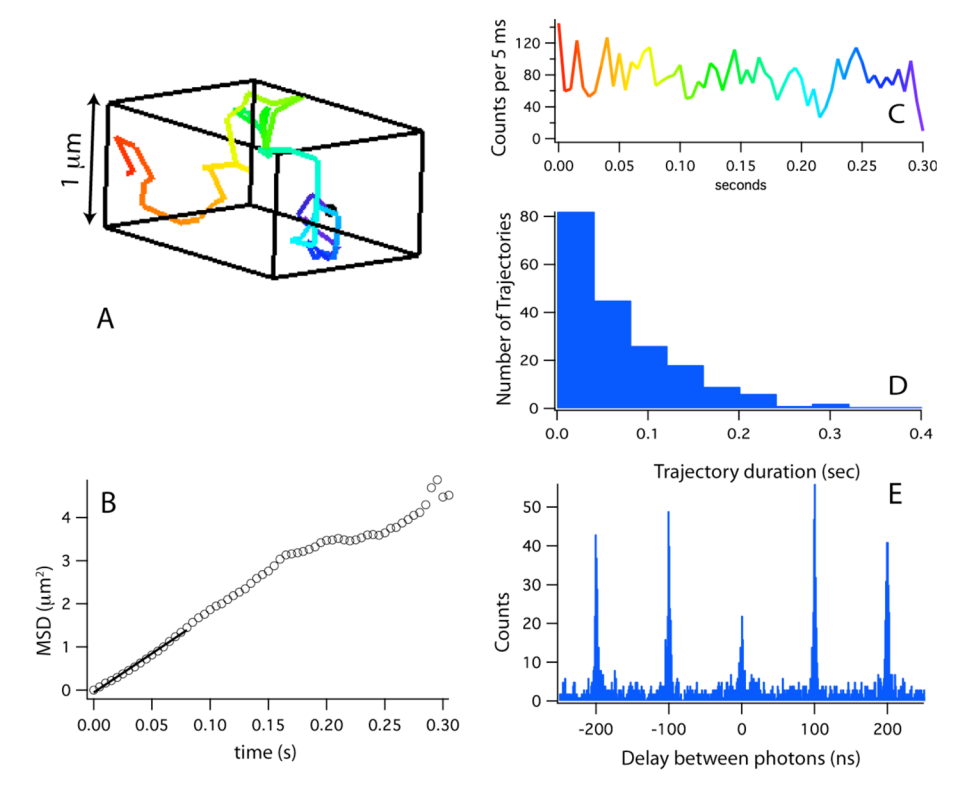


Figure 2. A. A 3D trajectory for a single Cy5-dUTP tracked in a 90/10 glycerol/water mixture. **B.** An analysis of the mean squared displacement (MSD) for this \sim 0.3 second-long trajectory. A linear fit (solid line) to the first $1/4^{th}$ of the trajectory returns a diffusion coefficient of \sim 3 μ m²/sec. **C.** Counts obtained during this 3D track. **D.** A histogram of track durations shows approximately 25% of the tracks last longer than 0.1 seconds. **E.** A photon-pair correlation histogram obtained by summing the pair correlations obtained from 50 tracks that lasted longer than 0.1 seconds. The observed photon anti-bunching behavior demonstrates these trajectories are from individual Cy5-dUTP molecules.

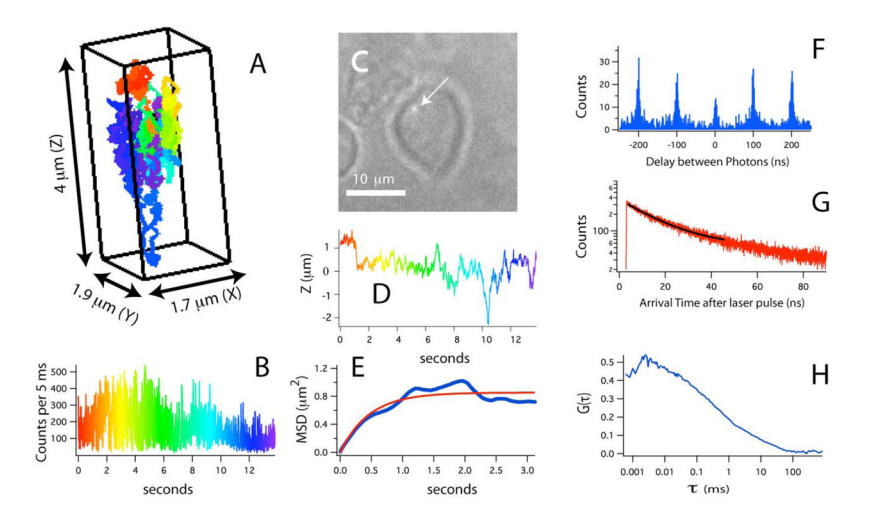


Figure 3. A. 3D trajectory of a single QD labeled IgE-FcεRI on an unstimulated mast cell at 37°C. A rainbow color scheme is used to denote the passage of time. **B.** The counts used for 3D tracking and feedback. **C.** A CCD image showing the receptor location relative to the mast cell. **D.** The Z-position of this receptor, showing over 4 μm of Z-motion that would be missed in CCD-based tracking methods. **E.** The mean squared displacement (blue) and fit (red). The motion is highly compartmentalized and is fit using Equation 3 of the supplementary material. **F.** A photon pair correlation measurement derived from this ~14 second long trajectory that shows fluorescence photon anti-bunching. **G.** A histogram of photon arrival times with respect to the excitation laser pulse (red) and exponential fit (black) which yields a 16 ns fluorescence lifetime **H.** An autocorrelation analysis of photon detection rate obtained during this trajectory. The decay in the correlation curve is dominated by quantum dot blinking dynamics.

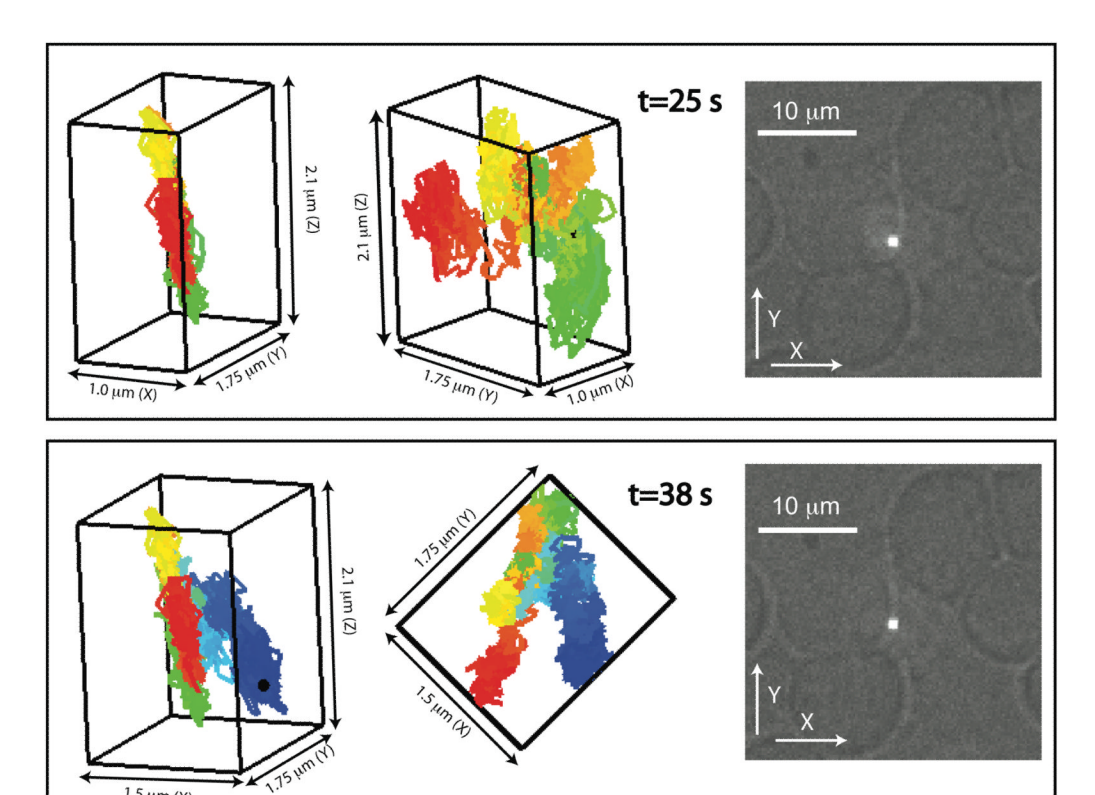


Figure 4.
Top: Two representations of a 3D trajectory QD-IgE-FcεRI taken 25 seconds into the trajectory and CCD image of the receptor position with respect to the cell. At this time, the trajectory is primarily 2D and is clearly on the side of the cell. Bottom: Later in the trajectory, this QD-IgE-FcεRI ventures perpendicularly outward from the main cell body.

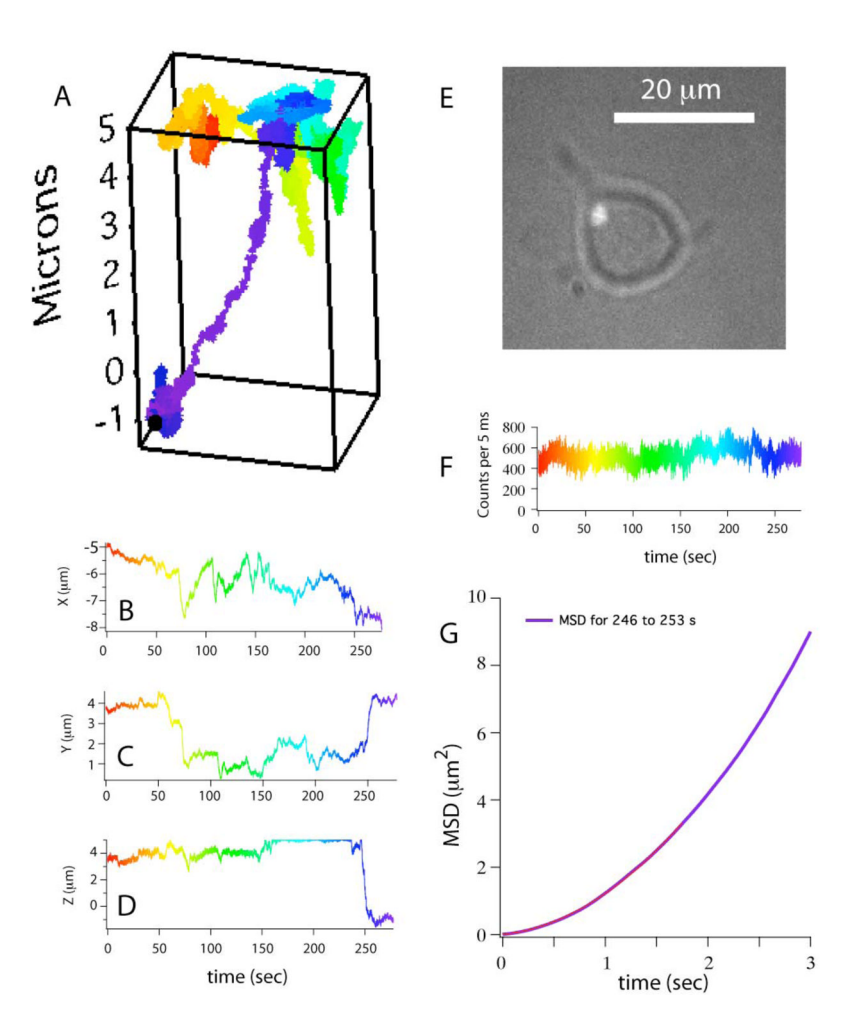


Figure 5. A. A 3D trajectory obtained from a single signaling patch of approximately 5 quantum dot labeled IgE-FcεRI. A rainbow color scheme is used to denote the passage of time. **B, C, D** show the X, Y, and Z position of this cluster. Between ~160–235 seconds the cluster is near the maximum travel of the piezo stage in the +Z dimension (+5 μm). While the cluster is at the maximum of our positive Z travel, it is not lost, as the counts do not significantly drop, the image of the cluster remains in focus (Sup. Movie M5), and we often give stage commands that move in the minus Z direction. **E.** The image of this cell obtained by the CCD camera near the beginning of the track. **F** The counts used for feedback and tracking. **G.** The MSD for 246–253 second period (purple) and fit (red). The MSD is parabolic, indicative of directed motion. A fit to the MSD using Equation 2 of the Supplementary Material yields a transport velocity of 950 nm/sec for the steep plunge occurring between 246 and 253 seconds.